Journal of Cerebral Blood Flow & Metabolism (2015) 35, 1454–1461

www.jcbfm.com

ORIGINAL ARTICLE

Role of lipocalin-2 in brain injury after intracerebral hemorrhage

Wei Ni, Mingzhe Zheng, Guohua Xi, Richard F Keep and Ya Hua

Lipocalin-2 (LCN2) is a siderophore-binding protein involved in cellular iron transport and neuroinflammation. Both iron and inflammation are involved in brain injury after intracerebral hemorrhage (ICH) and this study examined the role of LCN2 in such injury. Male adult C57BL/6 wild-type (WT) or LCN2-deficient ($LCN2^{-/-}$) mice had an intracerebral injection of autologous blood or $FeCl_2$. Control animals had a sham operation or saline injection. T2-weighted magnetic resonance imaging and behavioral tests were performed at days 1, 3, 7, 14, and 28 after injection. In WT mice, brain LCN2 levels were increased in the ipsilateral basal ganglia after ICH or iron injection. Lipocalin-2-positive cells were astrocytes, microglia, neurons, and endothelial cells. Intracerebral hemorrhage resulted in a significant increase in ferritin expression in the ipsilateral basal ganglia. Compared with WT mice, ICH caused less ferritin upregulation, microglia activation, brain swelling, brain atrophy, and neurologic deficits in $LCN2^{-/-}$ mice ($P < 0.05$). The size of the lesion induced by $FeCl_2$ injection as well as the degree of brain swelling and blood–brain barrier disruption were also less in $LCN2^{-/-}$ mice ($P < 0.05$). These results suggest a role of LCN2 in enhancing brain injury and iron toxicity after ICH.

Journal of Cerebral Blood Flow & Metabolism (2015) **35,** 1454–1461; doi:10.1038/jcbfm.2015.52; published online 8 April 2015

Keywords: blood–brain barrier; brain atrophy; intracerebral hemorrhage; iron; lipocalin-2

INTRODUCTION

Iron has a major role in brain damage after intracerebral hemorrhage (ICH).[1,2] Brain non-heme iron increases after ICH in rats and brain iron overload causes brain edema in the acute phase and brain atrophy later after ICH.[2,3] An iron chelator, deferoxamine, reduces ICH-induced brain edema, neuronal death, brain atrophy, and neurologic deficits in rats and pigs.[2–4] Clinical data also suggest a role of iron in ICH-induced brain injury. For example, clot lysis is associated with perihematomal edema development.[5] Recent studies showed that high levels of serum ferritin, an iron storage protein, are independently associated with poor outcome and severe brain edema in ICH patients.[6,7]

Lipocalin-2 (LCN2) is an acute phase protein that is upregulated in inflammation, infection, and a variety of injuries.[8] It binds siderophores, which are secreted by microorganisms to scavenge iron.[9] However, there is beginning to be evidence that LCN2 is involved in iron homeostasis. There is evidence that it can be involved in cellular uptake or clearance of iron depending on iron status.[10] Another report has suggested that LCN2 could be a mediator of an alternative, transferrin-independent pathway for cellular iron delivery.[11] In rats, LCN2 is upregulated after ICH and it may potentially have a role in handling iron that is released from the hematoma during clot resolution.[12] However, whether such a role is beneficial or detrimental is uncertain.

As an acute phase protein, LCN2 is also involved in inflammatory responses. Enhanced LCN2 expression was observed in choroid plexus and microvascular endothelial cells in brain parenchyma after peripheral lipopolysaccharide administration.[13] In cerebral ischemia, LCN2 contributed to neuronal cell death by promoting neurotoxic glial activation, neuroinflammation, and blood–brain barrier (BBB) disruption.[14] Lack of LCN2 also reduced inflammation resulting in less secondary damage and better locomotor recovery after spinal cord contusion injury.[15] Inflammation has an important role in ICH-induced brain injury.[16]

This study investigates the effect LCN2 deficiency on the expression of ferritin (an iron storage protein), microglia activation, neuronal death, and neurologic deficits in a mouse model of ICH. In addition, the role of LCN2 in iron-induced brain injury was also examined.

MATERIALS AND METHODS

Animal Preparation and Intracerebral Injection

All animal procedures were approved by the University Committee on Use and Care of Animals, University of Michigan. The University of Michigan has an Animal Welfare Assurance on file with the Office for Protection from Research Risks and is fully accredited by the American Association for the Accreditation of Laboratory Animal Care. The studies follow the Guide for The Care and Use of Laboratory Animals (National Research Council) and comply with the ARRIVE guidelines for reporting *in vivo* experiments. A total of 70 adult male C57BL/6 wild-type (WT) mice (Charles River Laboratories, Roanoke, IL, USA) and 43 male LCN2 knockout ($LCN2^{-/-}$) mice (University of Michigan Breeding Core) at age of 3 to 5 months were used. Two $LCN2^{-/-}$ mice died during anesthesia.

Intracerebral injections were performed as previously described.[17] Briefly, mice were anesthetized with ketamine (90 mg/kg, intraperitoneally, Abbott Laboratories, Chicago, IL, USA) and xylazine (5 mg/kg

Department of Neurosurgery, University of Michigan, Ann Arbor, Michigan, USA. Correspondence: Dr Ya Hua, R5018 BSRB, Department of Neurosurgery, University of Michigan, 109 Zina Pitcher Place, Ann Arbor, Michigan 48109-2200, USA.
E-mail: yahua@umich.edu
This study was supported by grants NS-073595, NS-079157, NS-084049, and NS-091545 from the National Institutes of Health (NIH). The content is solely the responsibility of the authors and does not necessarily represent the official views of the NIH. Drs Ni and Zheng contributed equally to this study.
Received 18 December 2014; revised 24 February 2015; accepted 2 March 2015; published online 8 April 2015

intraperitoneally, Lloyd Laboratories, Shenandoah, IA, USA). Body temperature was maintained at 37.5°C by a feedback-controlled heating pad. The mice were positioned in a stereotaxic frame (Model 500, Kopf Instruments, Tujunga, CA, USA) and a cranial burr hole (1 mm) was drilled near the right coronal suture 2.5 mm lateral to the midline. A 26-gauge needle was inserted stereotaxically into the right basal ganglia (coordinates: 0.2 mm anterior, 3.5 mm ventral, and 2.5 mm lateral to the bregma). Either 30 μL autologous whole blood or 10 μL of $FeCl_2$ (1 mmol/L) was infused at 2 μL/min by a microinfusion pump (Harvard Apparatus Inc, South Natick, MA, USA). Control animals had either a sham operation with a needle insertion or a 10-μL saline injection. After injection, the needle remained in position for 10 minutes to prevent reflux and then it was gently removed. The burr hole was filled with bone wax, and the skin incision was sutured closed.

Experimental Groups

The present study was divided into two parts. In the first part, WT or $LCN2^{-/-}$ mice had ICH ($n=27$ each group) and were euthanized at days 1, 3, or 28 after ICH ($n=11$ at day 1, $n=8$ at days 3 and 28). The harvested brains were used for histology ($n=4$ per group, per time point) and western blotting assays ($n=7$ per group at day 1, $n=4$ per group, per other time point). Control animals had only a needle insertion (WT, $n=24$; $LCN2^{-/-}$, $n=4$) and were also euthanized at days 1, 3, or 28 for histology (WT, $n=4$, per time point; $LCN2^{-/-}$, $n=4$ at day 1) or western blot (WT, $n=4$, per time point). In the second part, WT ($n=11$) and $LCN2^{-/-}$ ($n=10$) mice had 10 μL of $FeCl_2$ (1 mmol/L) injected into the right basal ganglia. Control WT mice ($n=8$) had 10 μL of saline injection. At 24 hours after the injections, mice underwent T2 magnetic resonance imaging (MRI) and they were then euthanized and the brains used for histology and western blotting assays.

Magnetic Resonance Imaging and Brain Swelling Measurement

Mice were anesthetized with 2% isoflurane/air mixture throughout MRI examination. Magnetic resonance imaging was performed at days 1, 3, 7, 14, and 28 in a 7.0-T Varian MR scanner (183-mm horizontal bore; Varian, Palo Alto, CA, USA) at the Center for Molecular Imaging of the University of Michigan including a T2 fast spin-echo (repetition time/echo time = 4,000/60 ms) using a field of view of 20 × 20 mm, matrix of 256 × 256 mm, and 25 coronal slices (0.5-mm thick). The images were preserved as 256 × 256 pixel pictures for brain swelling and T2 lesion calculation in NIH image J (Wayne Rasband, National Institutes of Health, USA). The calculation of brain swelling was based on seven every other sections whose center was the anterior commissure layer; the value was ((volume of ipsilateral hemisphere–volume of contralateral hemisphere)/volume of contralateral hemisphere) × 100%.

Immunohistochemistry and Brain Atrophy Measurement

Immunohistochemistry and immunofluorescence double staining were performed as described previously.[18] Briefly, mice were euthanized (ketamine 120 mg and xylazine 5 mg/kg intraperitoneally) and subjected to intracardiac perfusion with 4% paraformaldehyde in 0.1 mmol/L phosphate-buffered saline (pH 7.4). Brains were harvested and kept in 4% paraformaldehyde for 24 hours, then immersed in 30% sucrose for 3 to 4 days at 4°C. After embedding in a mixture of 30% sucrose and optimal cutting temperature compound (Sakura Finetek, Inc., Torrance, CA, USA) at a ratio of 1:2, the brain was sectioned on a cryostat into 18 μm slices and then preserved at − 80°C.

Hematoxylin and eosin (H&E) staining was used for caudate atrophy measurement at day 28. Three coronal sections from 0.5 mm posterior to the blood injection site were stained and photographed under a microscope (Olympus, BX51, Waltham, MA, USA) with × 1.25 magnification. The bilateral caudate were outlined in NIH image J and caudate size measured as described in the MRI method section. Brain atrophy was calculated as ((contralateral–ipsilateral caudate area)/ contralateral caudate area) × 100%.

Immunohistochemistry was performed as previously described.[19] The primary antibodies were polyclonal goat anti-LCN2 IgG (R&D System, Minneapolis, MN, USA, 1:200 dilution), polyclonal rabbit anti-ferritin IgG (AbD; 1:500 dilution), goat anti-albumin antibody (Bathyl Laboratories, Inc., Montgomery, TX, USA, 1:10,000 dilution) and polyclonal rabbit anti-ionized calcium-binding adaptor molecule 1 (Iba1) IgG (Wako, Richmond, VA, USA, 1:400 dilution). For immunofluorescence double labeling, the primary antibodies were polyclonal rabbit anti-glial fibrillary acidic protein (GFAP) IgG (Millipore, Billerica, MA, USA, 1:400 dilution), polyclonal rabbit anti-neuronal-specific nuclear protein (NeuN) IgG (Abcam, Cambridge, MA, USA, 1:500 dilution) and polyclonal rabbit anti-CD31 IgG (Abcam, 1:50 dilution), as well as those for LCN2 and Iba1. The secondary antibodies were Alexa Fluro 488-conjugated donkey anti-rabbit mAb (Invitrogen, 1:500 dilution) and Alexa Fluro 594-conjugated donkey anti-goat mAb (Invitrogen, Grand Island, NY, USA, 1:500 dilution). The double labeling was analyzed using a fluorescence microscope (Olympus, BX51).

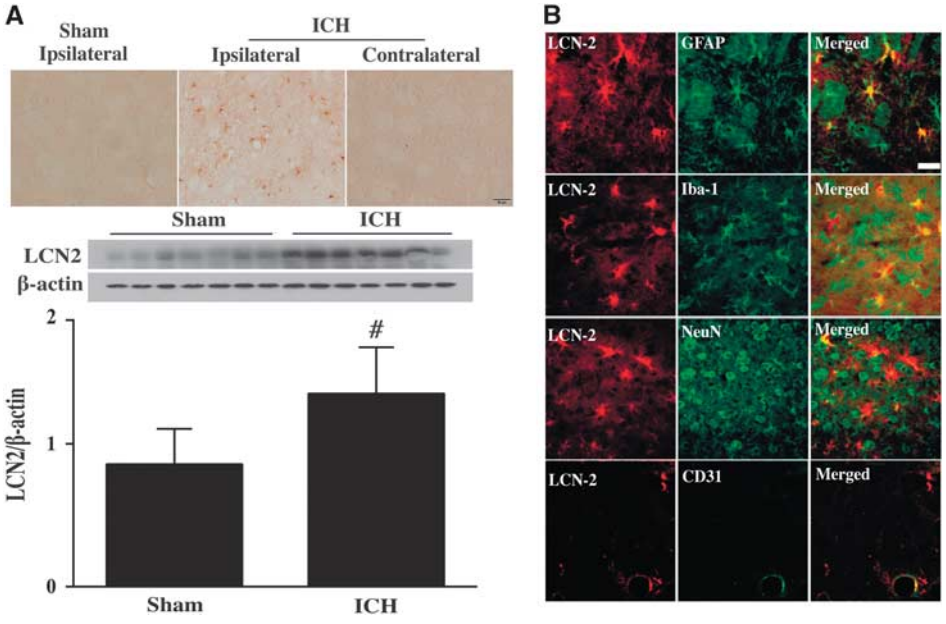

Figure 1. (**A**) Lipocalin 2 (LCN2) immunoreactivity in the ipsilateral basal ganglia after a sham operation, and in the contra- and ipsilateral basal ganglia of wild-type (WT) mice at 24 hours after intracerebral hemorrhage (ICH). Scale bar = 50 μm; and LCN2 protein levels in the ipsilateral basal ganglia at 24 hours after ICH or sham operation. Values (ratio to β-actin) are means ± s.d.; $n=7$ for each group, $^{\#}P<0.01$ versus the sham group. (**B**) Double labeling of LCN2 with GFAP (astrocyte marker), Iba-1 (microglia marker), NeuN (neuronal marker), and CD31 (endothelial marker) in the ipsilateral basal ganglia at 24 hours after ICH in WT mice. Scale bar = 20 μm.

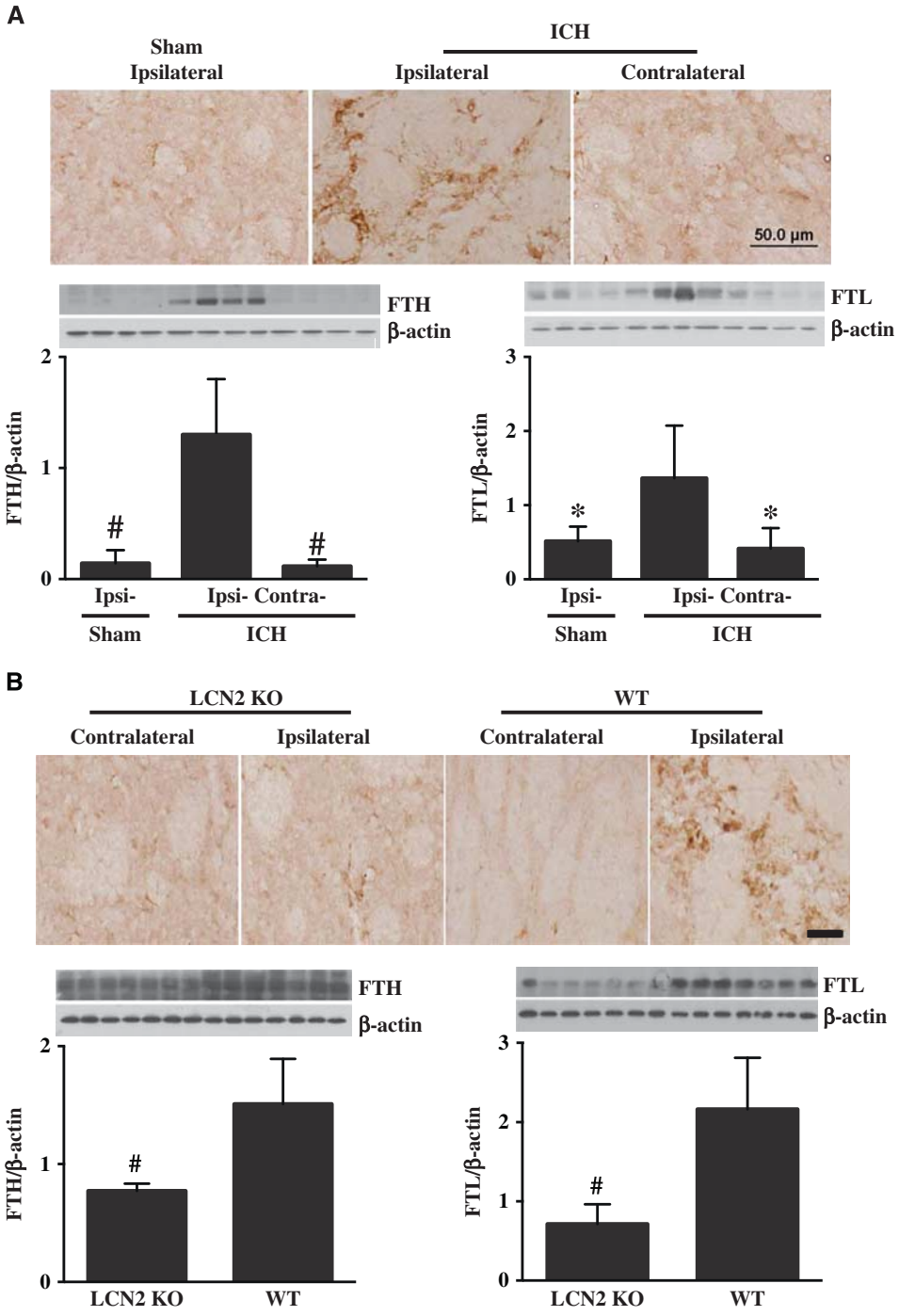

Figure 2. (**A**) Ferritin-positive cells, and the ferritin heavy chain (FTH) and light chain (FTL) protein levels in the basal ganglia at 24 hours after sham operation and intracerebral hemorrhage (ICH) in WT mice. Values (ratio to β-actin) are means ± s.d.; $n = 4$ for each group, $^{\#}P < 0.01$, $^{*}P < 0.05$ versus ipsilateral side after ICH. Scale bar = 50 μm. (**B**) Ferritin immunoreactivity, and FTH and FTL protein levels in the ipsilateral basal ganglia of lipocalin-2 knockout ($LCN2^{-/-}$) and WT mice at 24 hours after ICH. Values are means ± s.d.; $n = 7$ for each group, $^{\#}P < 0.01$ versus WT mice. Scale bar = 50 μm.

Western Blotting

Western blot analysis was performed as previously described.[18] Briefly, mice were perfused with 0.1 mmol/L phosphate-buffered saline (pH 7.4) after euthanasia, and the ipsi- and contralateral basal ganglia were sampled. Protein concentration was determined by Bio-Rad protein assay kit (Hercules, CA, USA), and 50 μg protein samples were separated by sodium dodecyl sulfate-polyacrylamide gel electrophoresis and transferred onto a hybond-C pure nitrocellulose membrane (Amersham, Pittsburgh, PA, USA). Membranes were probed with the following primary antibodies: polyclonal goat anti-LCN2 IgG (R&D System, 1:500 dilution), polyclonal rabbit anti-Iba1 IgG (Wako, 1:1,000 dilution), polyclonal goat anti-ferritin-L-chain IgG (FTL, Abnova, Walnut, CA, USA, 1:2,000 dilution), goat anti-albumin antibody (Bathyl Laboratories, Inc., 1:10,000 dilution), polyclonal rabbit anti ferritin-H-chain IgG (FTH, Cell Signaling, Beverly, MA, USA, 1:2,000

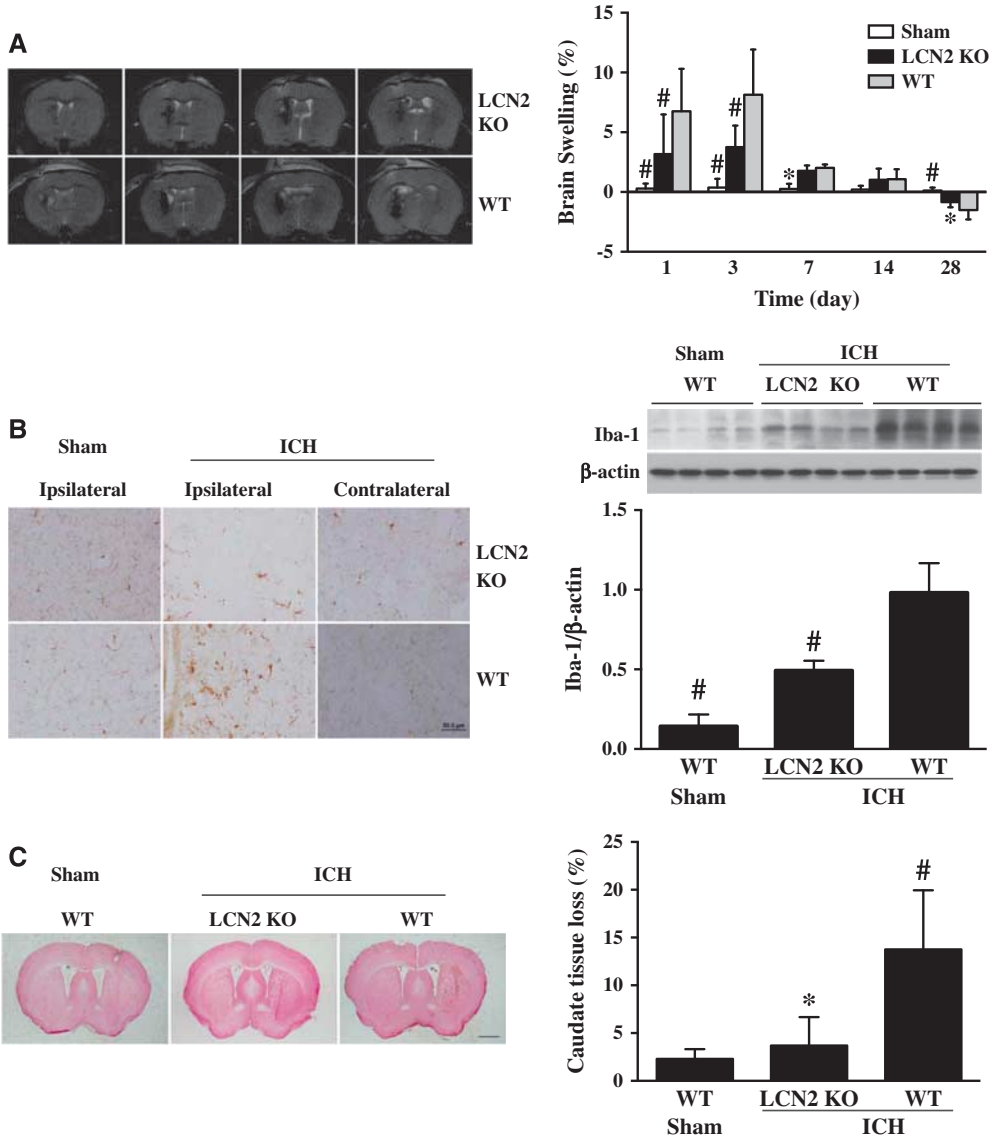

Figure 3. (**A**) T2-weighted magnetic resonance imaging (MRI) images at 24 hours after 30 μL blood was injected into the right basal ganglia in lipocalin-2 knockout (LCN2$^{-/-}$) or wild-type (WT) mice. Brain swelling calculated as ((ipsilateral–contralateral hemisphere)/contralateral hemisphere)) × 100% at days 1, 3, 7, 14, and 28 after blood injection in LCN2$^{-/-}$ or WT mice. Values are mean ± s.d.; $^{\#}P < 0.01$, $^{*}P < 0.05$ versus WT intracerebral hemorrhage (ICH) group. (**B**) Iba-1 immunoreactivity and protein levels in the basal ganglia of WT and LCN2$^{-/-}$ mice at 24 hours after ICH or sham operation, scale bar = 50 μm. Values are mean ± s.d.; $n = 4$ for each group, $^{\#}P < 0.01$, versus WT ICH group. (**C**) Ipsilateral caudate tissue loss at day 28 after 30 μL blood was injected into the right basal ganglia in LCN2$^{-/-}$ and WT mice. Tissue loss was calculated as ((contralateral–ipsilateral caudate)/contralateral caudate) × 100%. Values are mean ± s.d.; $n = 4$ for each group, $^{*}P < 0.05$, versus WT ICH group, scale bar = 1 mm.

dilution) and polyclonal rabbit anti β-actin IgG (Cell Signaling, 1:5,000 dilution). The secondary antibodies were goat anti-rabbit IgG and rabbit anti-goat IgG (1:2,000 dilution; Bio-Rad, Hercules, CA, USA). Antigen–antibody complexes were visualized with the ECL chemiluminescence system (Amersham) and exposed to Kodak X-OMAT film. The relative densities of bands were analyzed with NIH Image J.

Behavioral Tests

Forelimb use asymmetry and corner turn tests were used for behavioral evaluation.[20–22] For the forelimb use asymmetry, forelimb use during exploratory activity was analyzed in a transparent cylinder (10 cm in diameter and 13 cm in height). The following criteria were used for scoring: independent use of the left or right forelimb for contacting the wall during a full rear to initiate a weight-shifting movement and simultaneous use of both the left and right forelimbs to contact the wall. Behavior score was recorded by determining the number of times the ipsilateral (unimpaired) forelimb (*I*), contralateral forelimb (*C*), and both forelimbs (*B*) used as a percentage of total number of limb usage. A single, overall limb-use asymmetry score was calculated as follows: forelimb use asymmetry score = $(I - C)/(I+C+B)$. Corner turn test was performed as follows. The mouse was allowed to proceed into a corner with a 30° angle. When the mouse turned, its choice of direction (left or right) was recorded. Each mouse repeated this procedure for 20 times. The percentage of right turns was calculated.

Statistical Analysis

All the data in this study are presented as mean ± s.d. Data were analyzed by Student's *t*-test for single comparisons or ANOVA with *post hoc*

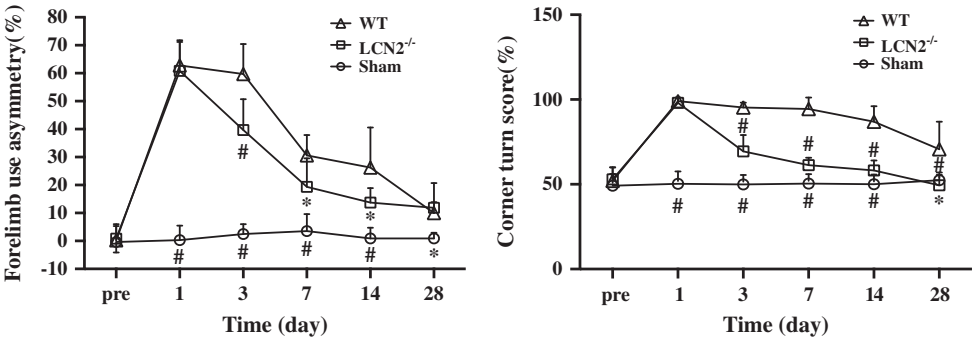

Figure 4. Forelimb use asymmetry and corner turn scores at days 1, 3, 7, 14, and 28 after a needle insertion or 30 μL blood injection into the right basal ganglia of lipocalin-2 knockout ($LCN2^{-/-}$) and wild-type (WT) mice. Values are mean ± s.d.; $^{\#}P < 0.01$, $^{*}P < 0.05$, versus WT group.

Bonferroni-Dunn correction for multiple comparisons. $P < 0.05$ was considered as statistically significant.

RESULTS

Brain Lipocalin-2 Upregulation after Intracerebral Hemorrhage

Intracerebral hemorrhage resulted in LCN2 upregulation in WT mice with many LCN2-positive cells detected in the ipsilateral basal ganglia at 24 hours after ICH. Few LCN2-positive cells were detected in the contralateral basal ganglia of ICH mice or the ipsilateral basal ganglia of sham mice (Figure 1A). Brain LCN2 protein levels in the ipsilateral basal ganglia were significantly higher in ICH mice compared with sham-operated mice at day 1 (LCN2/β-actin ratio: 1.34 ± 0.33 versus 0.85 ± 0.25 in the sham, $P < 0.05$, Figure 1A). Double labeling showed that LCN2 immunoreactivity colocalized with GFAP (an astrocyte marker), Iba-1 (a microglia marker), NeuN (a neuronal marker), and CD31 (an endothelial cell marker) immunoreactivity (Figure 1B).

Intracerebral Hemorrhage-induced Less Brain Ferritin Upregulation in Lipocalin-2 Knockout Mice

Our previous study in rats showed that ferritin, an iron storage protein, is upregulated in brain after ICH.[19] Similarly, in WT mice, numerous ferritin-positive cells were found in the perihematomal area at day 1 after ICH, but not in the contralateral basal ganglia or in the ipsilateral basal ganglia of sham-operated mice (Figure 2A). Western blots showed the protein levels of both FTH and FTL were higher in the ipsilateral basal ganglia versus that in sham mice at day 1 after ICH ($P < 0.05$; Figure 2A).

After ICH, there were no differences in ferritin immunoreactivity in the contralateral basal ganglia between WT and $LCN2^{-/-}$ mice, but there were far fewer ferritin-positive cells in the ipsilateral basal ganglia of $LCN2^{-/-}$ mice compared with WT mice at day 1 (Figure 2B). Western blots showed both FTH and FTL levels were lower in $LCN2^{-/-}$ mice (FTH/β-actin: 0.77 ± 0.06 versus 1.51 ± 0.38 in WT, $P < 0.01$; FTL/β-actin: 0.71 ± 0.25 versus 2.16 ± 0.65 in WT, $P < 0.01$; Figure 2B) at 24 hours after ICH.

Intracerebral Hemorrhage Caused Less Brain Swelling, Microglia Activation, and Brain Atrophy in Lipocalin-2 Knockout Mice

T2-weighted MRI was used to determine ICH-induced brain swelling in mice. A blinded observer outlined the hemisphere for each animal and measured the volume. Intracerebral hemorrhage caused brain swelling in WT mice at days 1, 3, and 7 compared with sham (e.g., day 3: 8.2 ± 3.8% versus 0.4 ± 0.7%, $P < 0.01$, Figure 3A). Less severe brain swelling was found in $LCN2^{-/-}$ mice compared with WT mice at day 1 (3.2 ± 3.3% versus 6.8 ± 3.6% in WT group, $P < 0.01$; Figure 3A) and day 3 (3.8 ± 1.8% versus 8.2 ± 3.8%, $P < 0.01$; Figure 3A). There was no brain swelling in either WT mice or $LCN2^{-/-}$ mice at days 14 and 28. In addition, the brain swelling ratio turned negative at day 28, indicating the brain atrophy after ICH in both WT and $LCN2^{-/-}$ groups.

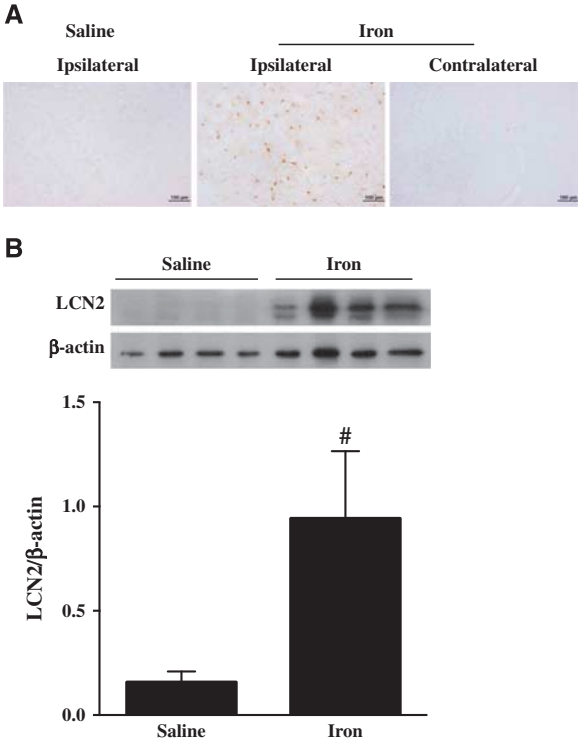

Figure 5. (**A**) Lipocalin-2 (LCN2) immunoreactivity at 24 hours in the basal ganglia of wild-type (WT) mice that had an intracaudate injection of either saline (10 μL) or $FeCl_2$ (10 μL, 1 mmol/L). Scale bar = 100 μm. (**B**) LCN2 protein levels in the ipsilateral basal ganglia of mice that had an intracaudate injection of either saline (10 μL) or $FeCl_2$ (10 μL, 1 mmol/L). Values are mean ± s.d., $n = 4$ for each group, $^{\#}P < 0.01$ versus saline group.

Intracerebral hemorrhage induces perihematomal microglial activation. There were more ameboid-shaped Iba-1-positive cells in the ipsilateral basal ganglia of WT mice 24 hours after ICH compared with the contralateral basal ganglia or sham-operated mice (Figure 3B). In contrast to the microglial activation in WT, there were fewer and thinner Iba-1-positive cells in the ipsilateral basal ganglia of $LCN2^{-/-}$ mice after ICH (Figure3B). These cells morphologically were less dendritic with round shape distinguished from activated microglia. Iba-1 protein levels in ipsilateral

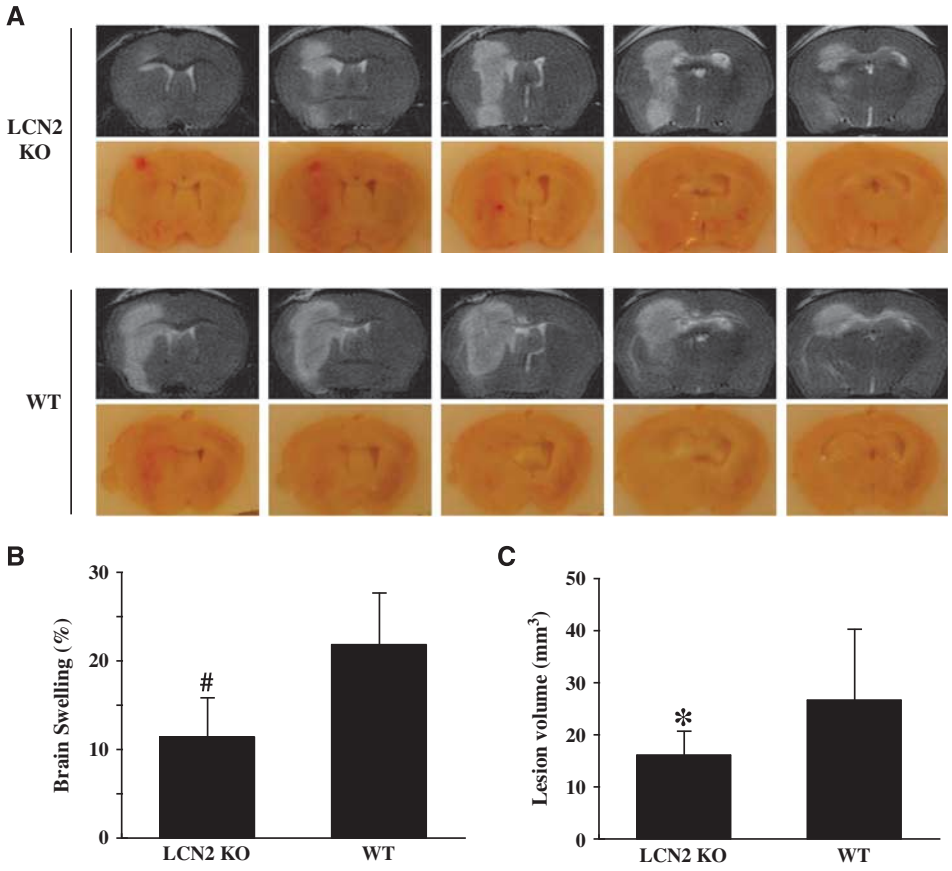

Figure 6. Comparison of brain injury in wild-type (WT) and lipocalin-2 knockout ($LCN2^{-/-}$) mice at 24 hours after 10 μL $FeCl_2$ (1 mmol/L) was injected into the right basal ganglia. (**A**) Coronal sections of T2 magnetic resonance imaging (MRI) images and the frozen sections of mouse brains. (**B**) Brain swelling: ((ipsilateral–contralateral hemisphere)/contralateral hemisphere) × 100%. Values are means ± s.d., $n = 10$ to 11 for each group, $^{\#}P < 0.01$ versus WT group. (**C**) MRI T2 lesion volumes. Values are mean ± s.d., $n = 10$ to 11 for each group, $^{*}P < 0.05$ versus WT group.

basal ganglia after ICH were significantly lower in $LCN2^{-/-}$ mice compared with WT mice (Iba-1/β-actin: 1.12 ± 0.27 versus 0.74 ± 0.18, $P < 0.01$; Figure 3B).

Brain atrophy was examined in H&E-stained coronal sections at day 28 after ICH. The ipsilateral caudate tissue loss was calculated as: ((contralateral caudate area–ipsilateral caudate area)/contralateral caudate area) × 100%. There was significantly lower loss in $LCN2^{-/-}$ mice compared with WT mice (3.7 ± 3.0% versus 13.8 ± 6.2%, $P < 0.01$, Figure 3C).

Intracerebral Hemorrhage Caused Less Neurologic Deficits in Lipocalin-2 Knockout Mice

Both group showed significant neurologic deficits as assessed by forelimb use asymmetry and corner turn test at day 1 after ICH. However, the $LCN2^{-/-}$ mice had less neurologic deficits for both forelimb use asymmetry score (e.g., day 3: 40 ± 11% versus 60 ± 11%, $P < 0.01$, Figure 4) and corner turn score (e.g., day 3: 69 ± 10% versus 95 ± 3%, $P < 0.01$, Figure 4).

Intracerebral Injection of Iron Caused Lipocalin-2 Upregulation

Given the role of iron in ICH-induced brain injury, the effects of iron on LCN2 were examined. Intracerebral $FeCl_2$ injection caused brain LCN2 upregulation. Lipocalin-2-positive cells were found in the ipsilateral, but not in the contralateral basal ganglia of WT mice after intracaudate injection of iron. Few LCN2-positive cells were found in the saline injection group (Figure 5A). In the ipsilateral basal ganglia, LCN2 protein levels were significantly higher in $FeCl_2$-injected mice than in saline-injected mice as determined by western blot (LCN2/β-actin: 0.94 ± 0.32 versus 0.15 ± 0.05, $P < 0.01$; Figure 3B). Double staining confirmed that the LCN2-positive cells were mostly astrocytes and microglia (data not shown).

Iron-Induced Smaller Magnetic Resonance Imaging T2 Lesions and Less Brain Swelling and Blood–Brain Barrier Disruption in Lipocalin-2 Knockout Mice

Intracerebral injection of $FeCl_2$ caused a MRI T2 lesion, brain swelling, and BBB disruption (Figure 6). Iron caused smaller T2 lesions in LCN2 knockout mice at 24 hours (16.0 ± 4.7 versus 26.6 ± 13.6 mm^3 in WT mice, $P < 0.05$, Figure 6). There was also less severe brain swelling in LCN2 knockout mice (11.4 ± 4.4% versus 21.9 ± 5.8% in WT mice, $P < 0.01$, Figure 6). The BBB disruption was examined by albumin western blot. It was hard to detect albumin leakage in the ipsilateral basal ganglia of saline-injected mice (Figure 7A). However, iron injection caused significant albumin leakage in the ipsilateral basal ganglia in WT mice, an effect that was significantly reduced in LCN2 knockout mice (5,844 ± 411 versus 7,901 ± 771 pixels in WT mice, $P < 0.05$, Figure 7B).

DISCUSSION

In this study, we evaluated the role of LCN2 in brain injury after ICH in mice. The major findings were (1) Brain LCN2 levels were increased in the caudate after ICH and intracerebral injection of

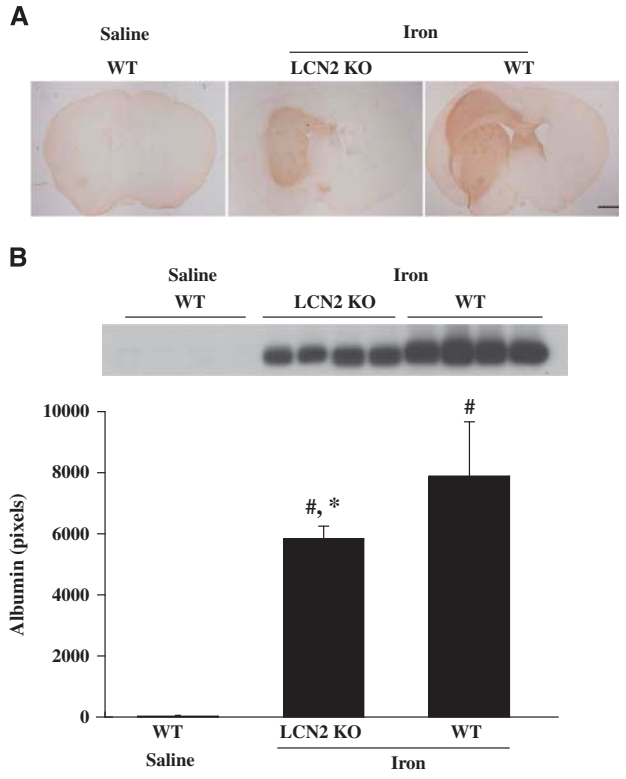

Figure 7. Albumin immunoreactivity (**A**) and protein levels (**B**) in the ipsilateral basal ganglia of WT and lipocalin-2 knockout ($LCN2^{-/-}$) mice that had 10 μL $FeCl_2$ (1 mmol/L) or saline injected into the right basal ganglia. Values are mean ± s.d., $n = 4$, $^{\#}P < 0.01$ versus WT saline group, $^{*}P < 0.05$ versus WT Iron group.

$FeCl_2$; (2) ICH-induced brain ferritin upregulation was less in LCN2 knockout mice; (3) ICH caused less microglial activation, brain swelling, brain atrophy, and neurologic deficits in LCN2 knockout mice; and (4) LCN2 deficiency resulted in smaller iron-induced lesions and less BBB disruption and brain swelling.

Expression of LCN2 was found in astrocytes, microglia, neurons, and endothelial cells after ICH in mice. Although LCN2 is considered as being mainly expressed in astrocytes,[12,14,23,24] where its secretion may be neurotoxic,[24] other cell types may express LCN2. Thus, inflammatory cells, such as microglia and neutrophils[15,25,26] can also express LCN2. The effects of LCN2 on microglia are complex. For example, LCN2 can increase the M1-related gene expression in cultured mouse microglia after 8 to 24 hours. Lipocalin-2 can also be secreted from M1-polarized microglia. Mice lacking LCN2 have a markedly reduced M1-related gene expression in microglia after lipopolysaccharide injection.[26] Expression of LCN2 was sensitive to cytotoxic agents, and inflammatory activation of microglia can lead to LCN2 upregulation. Meanwhile, LCN2 expression in BV-2 microglia induces cell morphologic changes. It induces a round shape with a loss of processes (the ameboid form) indicating activation.[25] In our present study, microglia activation after ICH was lower in LCN2 knockout than in WT mice. This difference in microglia activation may contribute to the difference in brain injury between WT and LCN2 knockout mice after ICH. Endothelial LCN2 may be involved in angiogenesis. Recent study showed LCN2 increased tube formation and cell migration in rat brain endothelial cells via iron and ROS-dependent mechanisms.[27]

The expression of ferritin after ICH is time dependent. In our previous paper in a rat model of ICH, FTL protein levels at day 1 were very low.[19] However, we still found iron- and ferritin-positive cells in the perihematomal zone as early as the first day. The protein level of FTH could also be detected at 24 hours. This indicates that cellular iron accumulation might start very early in the perihematomal zone after ICH. The source of iron could come from the serum and red blood cell lysis after ICH. In our mouse ICH model, we found that the FTL levels significantly increased at 24 hours. This more pronounced early upregulation compared with rat might be species related.

As well as inflammation, iron has a key role in ICH-induced brain injury. The current study showed that intracerebral injection of ferrous iron caused less brain injury, brain swelling, and BBB leakage in LCN2 knockout mice. Our previous findings showed that LCN2 was upregulated in a rat ICH model and that treatment with a ferric iron chelator, deferoxamine, attenuated ICH-induced LCN2 upregulation and brain injury.[12,28] Together, these results indicate that LCN2 has a role in iron-mediated brain injury after ICH. Until now, the detailed mechanism of iron delivery through LCN2 has not been fully elucidated. In the previous literatures, LCN2 was considered to be a mediator of an alternative, transferrin-independent pathway for cellular iron delivery.[11] Iron is suggested to bind an LCN2-associated small molecular weight siderophore, be transferred into cells through 24p3R, a LCN2 cell-surface receptor, and then be released resulting in an increased intracellular iron concentration.[10,29] The LCN2 deficiency can block the pathway of LCN2-reliant intracellular iron transportation, as suggested by the reduced iron-induced ferritin synthesis, and alleviate the brain injury. However, studies also showed that LCN2 can regulate the intracellular iron concentration and LCN2 deficiency can increase the cellular iron levels in sepsis.[30] Thus, the role of LCN2 in iron transport still need further study.

Advances have been made recently in identifying mammalian siderophores(s). In particular, recent evidence indicates that 2,5-DHBA (2,5-dihydroxy benzoic acid) is an important mammalian siderophore.[31,32] The role of 2,5-DHBA and the enzyme, 3-hydroxybutyrate dehydrogenase-2, involved in 2,5-DHBA biosynthesis needs to be evaluated in ICH.

The BBB disruption can contribute to brain edema after iron injection or ICH. The current study found less BBB leakage and brain swelling in LCN2 knockout mice compared with WT controls. Matrix metalloproteinase-9 (MMP-9) may contribute to the effect of LCN2 on BBB disruption. It is well known that MMP-9 can lead to BBB disruption[33,34] and LCN2 reduces MMP-9 degradation by forming an MMP-9/LCN2 complex.[35,36] Increasing the stability of MMP-9 may enhance the effect on BBB disruption. In addition, LCN2 may contribute to BBB disruption by enhancing microglia activation. Inflammation is an important regulator of BBB disruption in brain injury.

The current study shows that ICH-induced brain tissue loss is less in LCN2 knockout mice. The difference between LCN2 and WT mice reaction to ICH might relate to role of LCN2 in iron handling. Lipocalin-2 is considered to regulate iron uptake by binding to siderophores, with the resultant complex undergoing endocytosis after binding to cell-surface receptors, such as 24p3R.[10,37,38] Neurons, as well as astrocytes and endothelial cells, express the LCN2 receptor, 24p3R.[14] Based on this evidence, LCN2 knockout may decrease cellular iron uptake, alleviating iron-induced cell structure disruption and cell death. Indeed, we found ICH-induced upregulation of ferritin is less in LCN2 knockout mice, suggesting reduced cell iron concentrations.

In contrast to the effects of LCN2 deficiency on ferritin expression after ICH, we found no effect of the KO on ferritin levels in the contralateral hemisphere reflecting the very low levels of LCN2 in the normal brain. Targeting LCN2 after ICH may, therefore, have limited effects on normal brain tissue.

In conclusion, both ICH and intracerebral injection of iron caused upregulation of LCN2 in mouse brain and ICH/iron-induced brain injury was less in LCN2 knockout mice. The results suggest a role of LCN2 in brain injury after ICH.

DISCLOSURE/CONFLICT OF INTEREST

The authors declare no conflict of interest.

REFERENCES

1 Wagner KR, Sharp FR, Ardizzone TD, Lu A, Clark JF. Heme and iron metabolism: role in cerebral hemorrhage. *J Cereb Blood Flow Metab* 2003; **23**: 629–6652.
2 Xi G, Keep RF, Hoff JT. Mechanisms of brain injury after intracerebral haemorrhage. *Lancet Neurol* 2006; **5**: 53–63.
3 Keep RF, Hua Y, Xi G. Intracerebral haemorrhage: Mechanisms of injury and therapeutic targets. *Lancet Neurol* 2012; **11**: 720–731.
4 Xie Q, Gu Y, Hua Y, Liu W, Keep RF, Xi G. Deferoxamine attenuates white matter injury in a piglet intracerebral hemorrhage model. *Stroke* 2014; **45**: 290–292.
5 Wu G, Xi G, Huang F. Spontaneous intracerebral hemorrhage in humans: Hematoma enlargement, clot lysis, and brain edema. *Acta Neurochir* 2006; **96**: 78–80.
6 Perez de la Ossa N, Sobrino T, Silva Y, Blanco M, Millan M, Gomis M *et al.* Iron-related brain damage in patients with intracerebral hemorrhage. *Stroke* 2010; **41**: 810–813.
7 Mehdiratta M, Kumar S, Hackney D, Schlaug G, Selim M. Association between serum ferritin level and perihematoma edema volume in patients with spontaneous intracerebral hemorrhage. *Stroke* 2008; **39**: 1165–1170.
8 Jha MK, Lee S, Park DH, Kook H, Park KG, Lee IK *et al.* Diverse functional roles of lipocalin-2 in the central nervous system. *Neurosci Biobehav Rev* 2014; **49C**: 135–156.
9 Goetz DH, Holmes MA, Borregaard N, Bluhm ME, Raymond KN, Strong RK. The neutrophil lipocalin ngal is a bacteriostatic agent that interferes with siderophore-mediated iron acquisition. *Mol Cell* 2002; **10**: 1033–1043.
10 Devireddy LR, Gazin C, Zhu X, Green MR. A cell-surface receptor for lipocalin 24p3 selectively mediates apoptosis and iron uptake. *Cell* 2005; **123**: 1293–1305.
11 Yang J, Goetz D, Li JY, Wang W, Mori K, Setlik D *et al.* An iron delivery pathway mediated by a lipocalin. *Mol Cell* 2002; **10**: 1045–1056.
12 Dong M, Xi G, Keep RF, Hua Y. Role of iron in brain lipocalin 2 upregulation after intracerebral hemorrhage in rats. *Brain Res* 2013; **1505**: 86–92.
13 Marques F, Rodrigues AJ, Sousa JC, Coppola G, Geschwind DH, Sousa N *et al.* Lipocalin 2 is a choroid plexus acute-phase protein. *J Cereb Blood Flow Metab* 2008; **28**: 450–455.
14 Jin M, Kim JH, Jang E, Lee YM, Soo Han H, Woo DK *et al.* Lipocalin-2 deficiency attenuates neuroinflammation and brain injury after transient middle cerebral artery occlusion in mice. *J Cereb Blood Flow Metab* 2014; **34**: 1306–1314.
15 Rathore KI, Berard JL, Redensek A, Chierzi S, Lopez-Vales R, Santos M *et al.* Lipocalin 2 plays an immunomodulatory role and has detrimental effects after spinal cord injury. *J Neurosci* 2011; **31**: 13412–13419.
16 Wang J, Dore S. Inflammation after intracerebral hemorrhage. *J Cereb Blood Flow Metab* 2007; **27**: 894–908.
17 Nakamura T, Keep R, Hua Y, Schallert T, Hoff J, Xi G. Deferoxamine-induced attenuation of brain edema and neurological deficits in a rat model of intracerebral hemorrhage. *J Neurosurg* 2004; **100**: 672–678.
18 Xi G, Keep RF, Hua Y, Xiang J, Hoff JT. Attenuation of thrombin-induced brain edema by cerebral thrombin preconditioning. *Stroke* 1999; **30**: 1247–1255.
19 Wu J, Hua Y, Keep RF, Nakamura T, Hoff JT, Xi G. Iron and iron-handling proteins in the brain after intracerebral hemorrhage. *Stroke* 2003; **34**: 2964–2969.
20 Schallert T, Fleming SM, Leasure JL, Tillerson JL, Bland ST. Cns plasticity and assessment of forelimb sensorimotor outcome in unilateral rat models of stroke, cortical ablation, parkinsonism and spinal cord injury. *Neuropharmacology* 2000; **39**: 777–787.
21 Hua Y, Schallert T, Keep RF, Wu J, Hoff JT, Xi G. Behavioral tests after intracerebral hemorrhage in the rat. *Stroke* 2002; **33**: 2478–2484.
22 Nakamura T, Xi G, Hua Y, Schallert T, Hoff JT, Keep RF. Intracerebral hemorrhage in mice: Model characterization and application for genetically modified mice. *J Cereb Blood Flow Metab* 2004; **24**: 487–494.
23 Chia WJ, Dawe GS, Ong WY. Expression and localization of the iron-siderophore binding protein lipocalin 2 in the normal rat brain and after kainate-induced excitotoxicity. *Neurochem Int* 2011; **59**: 591–599.
24 Bi F, Huang C, Tong J, Qiu G, Huang B, Wu Q *et al.* Reactive astrocytes secrete lcn2 to promote neuron death. *Proc Natl Acad Sci USA* 2013; **110**: 4069–4074.
25 Lee S, Lee J, Kim S, Park JY, Lee WH, Mori K *et al.* A dual role of lipocalin 2 in the apoptosis and deramification of activated microglia. *J Immunol* 2007; **179**: 3231–3241.
26 Jang E, Lee S, Kim JH, Seo JW, Lee WH, Mori K *et al.* Secreted protein lipocalin-2 promotes microglial m1 polarization. *FASEB J* 2013; **27**: 1176–1190.
27 Wu L, Du Y, Lok J, Lo EH, Xing C. Lipocalin-2 enhances angiogenesis in rat brain endothelial cells via reactive oxygen species and iron-dependent mechanisms. *J Neurochem* 2015; **132**: 622–628.
28 Okauchi M, Hua Y, Keep RF, Morgenstern LB, Xi G. Effects of deferoxamine on intracerebral hemorrhage-induced brain injury in aged rats. *Stroke* 2009; **40**: 1858–1863.
29 Flo TH, Smith KD, Sato S, Rodriguez DJ, Holmes MA, Strong RK *et al.* Lipocalin 2 mediates an innate immune response to bacterial infection by sequestrating iron. *Nature* 2004; **432**: 917–921.
30 Srinivasan G, Aitken JD, Zhang B, Carvalho FA, Chassaing B, Shashidharamurthy R *et al.* Lipocalin 2 deficiency dysregulates iron homeostasis and exacerbates endotoxin-induced sepsis. *J Immunol* 2012; **189**: 1911–1919.
31 Liu Z, Ciocea A, Devireddy L. Endogenous siderophore 2,5-dihydroxybenzoic acid deficiency promotes anemia and splenic iron overload in mice. *Mol Cell Biol* 2014; **34**: 2533–2546.
32 Liu Z, Velpula KK, Devireddy L. 3-hydroxybutyrate dehydrogenase-2 and ferritin-h synergistically regulate intracellular iron. *FEBS J* 2014; **281**: 2410–2421.
33 Rosell A, Cuadrado E, Ortega-Aznar A, Hernandez-Guillamon M, Lo EH, Montaner J. Mmp-9-positive neutrophil infiltration is associated to blood-brain barrier breakdown and basal lamina type iv collagen degradation during hemorrhagic transformation after human ischemic stroke. *Stroke* 2008; **39**: 1121–1126.
34 Yang Y, Rosenberg GA. Mmp-mediated disruption of claudin-5 in the blood-brain barrier of rat brain after cerebral ischemia. *Methods Mol Biol* 2011; **762**: 333–345.
35 Kubben FJ, Sier CF, Hawinkels LJ, Tschesche H, van Duijn W, Zuidwijk K *et al.* Clinical evidence for a protective role of lipocalin-2 against mmp-9 autodegradation and the impact for gastric cancer. *Eur J Cancer* 2007; **43**: 1869–1876.
36 Yan L, Borregaard N, Kjeldsen L, Moses MA. The high molecular weight urinary matrix metalloproteinase (mmp) activity is a complex of gelatinase b/mmp-9 and neutrophil gelatinase-associated lipocalin (ngal). Modulation of mmp-9 activity by ngal. *J Biol Chem* 2001; **276**: 37258–37265.
37 Hvidberg V, Jacobsen C, Strong RK, Cowland JB, Moestrup SK, Borregaard N. The endocytic receptor megalin binds the iron transporting neutrophil-gelatinase-associated lipocalin with high affinity and mediates its cellular uptake. *FEBS Lett* 2005; **579**: 773–777.
38 Mori K, Lee HT, Rapoport D, Drexler IR, Foster K, Yang J *et al.* Endocytic delivery of lipocalin-siderophore-iron complex rescues the kidney from ischemia-reperfusion injury. *J Clin Investig* 2005; **115**: 610–621.